^{31}P and ^{195}Pt NMR Studies on the Clusters $[Pt_4(\mu_2\text{-}CO)_5L_4]$. L = PEt_3, PMe_2Ph, $PMePh_2$, PEt_2Bu^t. The Molecular Structure of a Monoclinic Modification of $[Pt_4(\mu_2\text{-}CO)_5(PMe_2Ph)_4]$.

ALFRED MOOR, PAUL S. PREGOSIN, LUIGI M. VENANZI

Laboratorium für Anorganische Chemie, ETH Zürich, Universitätstrasse 6, CH-8092 Zürich, Switzerland

and ALAN J. WELCH

Dewar Crystallographic Laboratory, Department of Chemistry, University of Edinburgh, Edinburgh EH9 3JJ, U.K.

Received July 9, 1983

Several cluster complexes of composition $[Pt_4(\mu_2\text{-}CO)_5L_4]$ have been synthesized and characterized, using ^{31}P and ^{195}Pt NMR. L = PEt_3, PMe_2Ph, $PMePh_2$, PEt_2Bu^t. The molecular structure of a new monoclinic modification of the PMe_2Ph derivative has been determined: space group $P2_1/n$ with a = 19.698(4), b = 10.9440(20), and c = 21.360(6) Å, β = 112.432(18)°, Z = 4. Using 4751 reflections measured at 290 ± 1 K on a four-circle diffractometer the structure has been refined to R = 0.0846. The molecule has no imposed symmetry, but the central $Pt_4(CO)_5P_4$ core has the approximate C_{2v} architecture established for the previously known orthorhombic modification. The Pt_4 unit is thus a highly distorted, edge-opened (3.3347 Å) tetrahedron, with five edge-bridging carbonyl and four terminal phosphine ligands. In contrast to the crystallographic results ^{31}P and ^{195}Pt NMR spectra reveal equivalent ^{31}P and ^{195}Pt spins, which can be interpreted in terms of a tetrahedral arrangement of platinum atoms. It is suggested that this equivalence arises from time-averaging of all possible isomeric edge-opened tetrahedra.

Introduction

There is continuing interest in the cluster chemistry of platinum [1], aided in part by the novel heterometallic clusters reported by Stone and co-workers, [2], and Braunstein and co-workers, [3]. In our previous studies we have analysed ^{31}P and ^{195}Pt NMR spectra for complexes of the type $[Pt_3(\mu_2\text{-}CO)_3L_3]$, *333*, [4], and $[Pt_3(\mu_2\text{-}CO)_3L_4]$, *334*, [5], where L is a tertiary phosphine ligand, and found interesting spectroscopic trends in the coupling constants $^1J(^{195}Pt,^{31}P)$, $^1J(^{195}Pt,^{195}Pt)$ and $^2J(^{195}Pt,^{31}P)$. In the course of these studies we obtained the known tetranuclear cluster complexes $[Pt_4(\mu_2\text{-}CO)_5L_4]$, *454*, and report here *a*) syntheses of some new members of this class of compounds *b*) their ^{31}P and ^{195}Pt NMR characteristics, including aspects of their solution dynamics and *c*) the X-ray structure of a crystalline modification of $[Pt_4(\mu_2\text{-}CO)_5(PMe_2Ph)_4]$, which differs from that previously reported [6].

Results and Discussion

The purple to dark-violet complexes $[Pt_4(\mu_2\text{-}CO)_5L_4]$, *454*, L = PEt_3, PEt_2Bu^t, and $PMePh_2$, were prepared in yields of 43–65% starting from $[Pt(1,5\text{-}COD)_2]$, C_2H_4, CO and the tertiary phosphine. The cluster with L = PMe_2Ph was obtained from the *334* cluster and CO. Initially, there was some question as to whether the previously obtained sample of $[Pt_4(\mu_2\text{-}CO)_5(PMe_2Ph)_4]$, described as orange-brown needles [6], was structurally identical to our sample since we obtained this complex as purple plates. Moreover, the solid state IR spectra for the two samples differed in the carbonyl stretching region in that the orange material showed bands at 1836(w), 1802(s) and 1780(vs) cm^{-1}, but the purple solid revealed three strong signals at 1800, 1784 and 1768 cm^{-1}. However, both samples gave purple solutions in toluene with identical spectra (1790, 1745 cm^{-1}). Since X-ray diffraction studies of $[Pt_4(\mu_2\text{-}CO)_5(PMe_2Ph)_4]$ revealed a 'butterfly' structure with two platinum environments [6], whereas the ^{31}P NMR spectrum of our sample showed the presence of magnetically equivalent phosphorus and platinum atoms (see later), the crystal structure of the purple modification of $[Pt_4(\mu_2\text{-}CO)_5(PMe_2Ph)_4]$ was determined.

X-Ray Crystal Structure of $[Pt_4(\mu_2\text{-}CO)_5(PMe_2Ph)_4]$

An ORTEP plot for a single molecule of $[Pt_4(\mu_2\text{-}CO)_5(PMe_2Ph)_4]$ is given in Fig. 1, and Tables I and II list some interatomic distances (uncorrected for thermal effects) and selected interbond angles, respectively. Positional and thermal parameters are shown in Table III.

0020-1693/84/$3.00

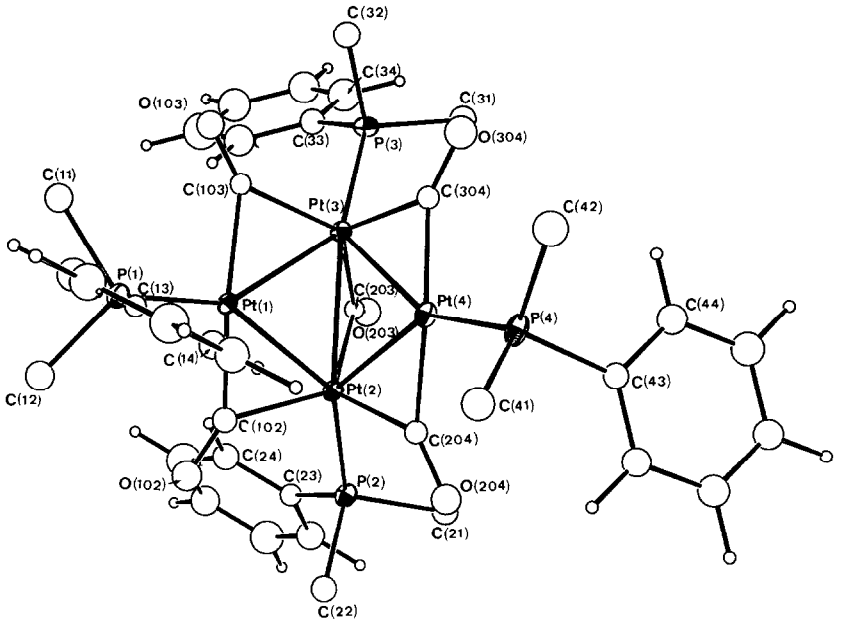

Fig. 1. Perspective view and atomic numbering scheme of $[Pt_4(\mu_2\text{-}CO)_5(PMe_2Ph)_4]$. Thermal ellipsoids are constructed at the 30% electron probability level, except for H atoms which have an artificial radius of 0.1 Å for clarity.

TABLE I. Interatomic Distances (Å).

Pt(1)–Pt(2)	2.7280(14)	Pt(1)–P(1)	2.233(6)
Pt(1)–Pt(3)	2.7064(15)	Pt(2)–P(2)	2.271(7)
Pt(2)–Pt(3)	2.7312(14)	Pt(3)–P(3)	2.261(6)
Pt(2)–Pt(4)	2.7537(15)	Pt(4)–P(4)	2.246(6)
Pt(3)–Pt(4)	2.7537(13)		
		P(1)–C(11)	1.866(29)
Pt(1)–C(102)	1.970(28)	P(1)–C(12)	1.826(31)
Pt(2)–C(102)	2.176(28)	P(1)–C(13)	1.819(18)
Pt(1)–C(103)	2.057(24)	P(2)–C(21)	1.893(31)
Pt(3)–C(103)	2.145(24)	P(2)–C(22)	1.822(29)
Pt(2)–C(203)	2.080(23)	P(2)–C(23)	1.820(22)
Pt(3)–C(203)	2.035(23)	P(3)–C(31)	1.806(32)
Pt(2)–C(204)	2.108(24)	P(3)–C(32)	1.809(31)
Pt(4)–C(204)	1.981(25)	P(3)–C(33)	1.852(26)
Pt(3)–C(304)	2.170(24)	P(4)–C(41)	1.812(34)
Pt(4)–C(304)	1.968(25)	P(4)–C(42)	1.854(38)
		P(4)–C(43)	1.820(19)
C(102)–O(102)	1.145(32)		
C(103)–O(103)	1.110(27)		
C(203)–O(203)	1.192(29)	Pt(1)···Pt(4)	3.3347(12)
C(204)–O(204)	1.224(29)		
C(304)–O(304)	1.203(31)		

The molecule may be thought of as an edge-opened tetrahedral cluster of four Pt atoms with four terminal PMe_2Ph ligands and five edge-bridging carbonyl groups. A different crystalline modification of this cluster was structurally characterized by Vranka *et al.* some years ago [6]. These authors reported that the cell is orthorhombic, with space group *Pcmn*, with $a = 19.96$, $b = 20.29$ and $c = 10.66$ Å, $U = 4317$ Å^3, and $Z = 4$, whilst ours is monoclinic, $P2_1/n$, with $a = 19.698(4)$, $b = 10.9440(20)$, and $c = 21.360(6)$ Å, $\beta = 112.432(18)°$, $U = 4256(3)$ Å, and $Z = 4$.

At a molecular level the present structure differs in *conformation* from that previously described. The orange modification sits on a crystallographic mirror plane through atoms Pt(3) and Pt(2), their bridging carbonyl function, and their terminal phosphine ligands. Our molecule has no imposed symmetry although the effective C_{2v} symmetry of the $\{Pt_4C_4P_4\}$-framework found for the orthorhombic modification is also apparent in the present study. It should be noted that the effective symmetry of both modifications is C_s, but is in the purple form about a mirror plane through Pt(1), Pt(4) and their phosphines, *i.e.* perpendicular to that found in the orange form. In summary, the two determined conformations differ mainly with respect to rotations about the Pt–P and P–C bonds.

Apart from differences in the overall shapes of the two modifications, there are some significant differences in molecular dimensions within the central cores. Notably, both the Pt(1)–Pt(2) and Pt(1)–Pt(3) distances, 2.7284(14) and 2.7064(15) Å, are substantially shorter than their chemical equivalents, Pt(4)–Pt(2) and Pt(4)–Pt(3) 2.7537(15) and 2.7577(13) Å, respectively, and the chemically unique Pt(2)–Pt(3) connectivity is intermediate in length, 2.7312(14) Å [*c.f.* Pt(1)–Pt(2 or 3) = Pt(4)–Pt(2 or 3) = 2.750(6) and 2.754(6) Å; Pt(3)–Pt(4) = 2.790(7) Å in the orthorhombic modification]. The most pronounced difference between the two structures is the non-bonding Pt(1)···Pt(4) distance; *i.e.*,

TABLE II. Selected Interbond Angles (°).

Pt(2)–Pt(1)–Pt(3)	60.34(4)	Pt(1)–C(102)–Pt(2)	82.1(11)
Pt(1)–Pt(2)–Pt(3)	59.44(4)	Pt(1)–C(102)–O(102)	146.1(24)
Pt(2)–Pt(3)–Pt(1)	60.22(4)	Pt(2)–C(102)–O(102)	130.2(23)
Pt(2)–Pt(4)–Pt(3)	59.46(4)	Pt(1)–C(103)–Pt(3)	80.2(8)
Pt(3)–Pt(2)–Pt(4)	60.27(4)	Pt(1)–C(103)–O(103)	141.5(21)
Pt(2)–Pt(3)–Pt(4)	60.27(4)	Pt(3)–C(103)–O(103)	138.1(21)
		Pt(2)–C(203)–Pt(3)	83.2(9)
P(1)–Pt(1)–Pt(2)	150.3(2)	Pt(2)–C(203)–O(203)	135.8(20)
P(1)–Pt(1)–Pt(3)	149.3(2)	Pt(3)–C(203)–O(203)	141.0(20)
P(4)–Pt(4)–Pt(2)	145.9(2)	Pt(2)–C(204)–Pt(4)	84.6(9)
P(4)–Pt(4)–Pt(3)	154.7(2)	Pt(2)–C(204)–O(204)	130.5(20)
P(2)–Pt(2)–Pt(1)	143.8(2)	Pt(4)–C(204)–O(204)	144.2(20)
P(2)–Pt(2)–Pt(3)	145.9(2)	Pt(3)–C(304)–Pt(4)	83.3(9)
P(2)–Pt(2)–Pt(4)	135.0(2)	Pt(3)–C(304)–O(304)	132.5(20)
P(3)–Pt(3)–Pt(1)	143.5(2)	Pt(4)–C(304)–O(304)	144.1(20)
P(3)–Pt(3)–Pt(2)	146.6(2)		
P(3)–Pt(3)–Pt(4)	134.0(2)	Pt(1)–P(1)–C(11)	115.0(10)
		Pt(1)–P(1)–C(12)	117.2(10)
C(102)–Pt(1)–Pt(2)	52.2(8)	Pt(1)–P(1)–C(13)	115.7(5)
C(102)–Pt(2)–Pt(1)	45.7(7)	C(11)–P(1)–C(12)	102.6(14)
C(103)–Pt(1)–Pt(3)	51.3(7)	C(11)–P(1)–C(13)	104.1(11)
C(103)–Pt(3)–Pt(1)	48.5(6)	C(12)–P(1)–C(13)	100.1(12)
C(203)–Pt(2)–Pt(3)	47.7(6)	Pt(2)–P(2)–C(21)	113.0(10)
C(203)–Pt(3)–Pt(2)	49.1(6)	Pt(2)–P(2)–C(22)	115.4(10)
C(204)–Pt(2)–Pt(4)	45.7(7)	Pt(2)–P(2)–C(23)	116.6(6)
C(204)–Pt(4)–Pt(2)	49.7(7)	C(21)–P(2)–C(22)	100.8(13)
C(304)–Pt(3)–Pt(4)	45.2(6)	C(21)–P(2)–C(23)	106.4(11)
C(304)–Pt(4)–Pt(3)	51.5(7)	C(22)–P(2)–C(23)	103.0(12)
		Pt(3)–P(3)–C(31)	113.0(10)
P(1)–C(13)–C(14)	119.0(5)	Pt(3)–P(3)–C(32)	114.1(10)
P(1)–C(13)–C(18)	121.0(5)	Pt(3)–P(3)–C(33)	116.1(7)
P(2)–C(23)–C(24)	118.1(5)	C(31)–P(3)–C(32)	103.7(14)
P(2)–C(23)–C(28)	121.7(5)	C(31)–P(3)–C(33)	106.4(12)
P(3)–C(33)–C(34)	120.7(6)	C(32)–P(3)–C(33)	102.2(12)
P(3)–C(33)–C(38)	119.1(6)	Pt(4)–P(4)–C(41)	113.2(11)
P(4)–C(43)–C(44)	117.0(5)	Pt(4)–P(4)–C(42)	116.2(12)
P(4)–C(43)–C(48)	123.0(5)	Pt(4)–P(4)–C(43)	112.1(7)
		C(41)–P(4)–C(42)	104.6(16)
		C(41)–P(4)–C(43)	106.0(12)
		C(42)–P(4)–C(43)	103.9(13)

TABLE III. Positional[a] and Thermal[b] Parameters.

Atom	*x*	*y*	*z*	*U*
Pt(1)[c]	−4023(5)[d]	22029(9)	−19962(4)	*
Pt(2)	10132(5)	22100(9)	−19168(4)	*
Pt(3)	1941(5)	43004(9)	−22246(5)	*
Pt(4)	10119(5)	37348(10)	−8918(5)	*
P(1)	−1353(3)	1226(6)	−1900(3)	*
P(2)	1876(3)	1077(7)	−2116(3)	*
P(3)	−67(4)	6060(6)	−2825(3)	*
P(4)	1444(4)	4050(8)	232(3)	*
C(102)	241(14)	786(27)	−1922(13)	51(7)[e]
O(102)	271(12)	−250(22)	−1979(11)	74(6)
C(103)	−910(13)	3845(21)	−2254(11)	36(5)
O(103)	−1461(11)	4281(19)	−2551(10)	64(5)
C(203)	923(13)	3615(21)	−2600(11)	35(5)
O(203)	1187(12)	3842(20)	−3003(11)	76(6)
C(204)	1623(14)	2283(23)	−864(12)	42(6)
O(204)	2162(11)	1698(20)	−508(10)	70(6)
C(304)	453(13)	5235(23)	−1265(12)	40(6)
O(304)	302(13)	6235(22)	−1123(11)	82(7)
C(11)	−2271(16)	1897(27)	−2401(14)	61(8)
C(12)	−1477(17)	−380(28)	−2149(15)	64(8)
C(13)	−1340(7)	1112(17)	−1045(8)	32(5)
C(14)	−675[f]	1267	−496	52(7)
C(15)	−653	1198	163	75(9)
C(16)	−1295	971	274	93(12)
C(17)	−1960	815	−275	81(10)
C(18)	−1982	886	−935	72(9)
C(21)	2812(17)	1831(28)	−1798(15)	63(8)
C(22)	2099(16)	−381(26)	−1672(14)	56(7)
C(23)	1674(9)	648(20)	−2992(11)	45(6)
C(24)	939	545	−3427	68(9)
C(25)	758	129	−4089	123(16)
C(26)	1313	−184	−4314	91(11)
C(27)	2048	−82	−3879	119(15)
C(28)	2228	335	−3218	81(10)
C(31)	686(17)	7135(29)	−2551(15)	65(8)
C(32)	−822(17)	6911(28)	−2757(15)	62(8)
C(33)	−351(13)	5905(19)	−3754	61(8)
C(34)	−148	6781	−4124	106(13)
C(35)	−415	6705	−4829	102(13)
C(36)	−885	5754	−5164	114(14)
C(37)	−1088	4879	−4793	132(17)
C(38)	−821	4955	−4088	90(11)
C(41)	1342(18)	2733(31)	702(17)	73(9)
C(42)	1020(21)	5326(34)	525(18)	87(11)
C(43)	2419(9)	4418(15)	575	46(6)
C(44)	2610	5628	519	66(8)
C(45)	3347	5979	784	83(10)
C(46)	3892	5118	1104	67(8)
C(47)	3700	3907	1159	73(9)
C(48)	2964	3557	895	62(8)

*These atoms refined anisotropically[g], producing:

Atom	U_{11}	U_{22}	U_{33}	U_{12}	U_{13}	U_{23}
Pt(1)	259(5)	382(5)	342(5)	−13(4)	158(4)	15(4)
Pt(2)	278(5)	404(5)	351(5)	19(4)	165(4)	−4(4)
Pt(3)	319(5)	374(5)	381(5)	14(4)	185(4)	32(4)
Pt(4)	359(6)	524(7)	297(5)	−38(5)	138(4)	−42(4)
P(1)	35(4)	47(4)	41(3)	−2(3)	21(3)	0(3)
P(2)	33(4)	53(4)	43(4)	1(3)	21(3)	−1(3)
P(3)	47(4)	39(4)	45(4)	8(3)	27(3)	10(3)
P(4)	39(4)	80(5)	29(3)	−8(4)	11(3)	−6(3)

[a]Positional parameters are in fractional co-ordinates of the unit cell edges, ×10^5 for Pt and ×10^4 for other atoms. [b]Thermal parameters are in Å^2, ×10^4 for Pt, ×10^3 for other atoms. [c]Atomic numbering scheme: P(i) is bound to Pt(i). CO(iOj) bridges Pt(i) and Pt(j). C(i1) and C(i2) are methyl carbons on P(i), and C(i3)–C(i8) are phenyl carbons, numbered cyclically, with C(i3) bound to P(i). [d]Estimated standard deviations, shown in parentheses throughout this paper, are right-adjusted to the least significant digit in the preceeding number. [e]The isotropic temperature factor is in the form $\exp\{-8\pi^2 U(\sin^2\theta)/\lambda^2\}$. [f]Phenyl rings refined as rigid bodies, hence errors in fractional coordinates are common. [g]The anisotropic thermal parameter is in the form $\exp\{-2\pi^2(U_{11}a^{*2}h^2 + U_{22}b^{*2}k^2 + U_{33}c^{*2}l^2 + 2U_{12}a^*b^*hk + 2U_{13}a^*c^*hl + 2U_{23}b^*c^*kl)\}$.

3.3347(12) Å in our compound *vs* 3.543(8) Å in the orange modification.

Using a simple description of the present cluster which envisages 16e configurations for Pt(1) and Pt(4), and 18e configurations for Pt(2) and Pt(3), one should be able to compare the four locally-equivalent Pt–Pt bond lengths with other carbonyl-bridged distances containing 16e and 18e Pt atoms, *eg* 2.736(1) and 2.714(1) Å in $[Pt_3(\mu_2\text{-}CO)_3\{P(C_6H_{11})_3\}_4]$ [7], rather than the more numerous, but generally shorter, CO-bridged distances between two 16e Pt centres, *eg* 2.653(2) and 2.656(2) Å in $[Pt_3(\mu_2\text{-}CO)_3\{P(C_6H_{11})_3\}_3]$ [8].

The Pt_3 triangles of the present molecule are almost orthogonal (dihedral angle 89.4°), and the peripheral carbonyl bridges all lean slightly towards the open tetrahedral edge (angles between adjacent Pt_3 and Pt_2 C-triangles span the range 6.4–10.2°). Furthermore, all four peripheral carbonyls bridge asymmetrically their Pt–Pt edges, consistently favouring the relatively electron-deficient atoms Pt(1) and Pt(4). Although the experimental errors concerned with the Pt–C distances in the present structure render this asymmetry barely significant, the same effect occurs in $[Pt_3(\mu_2\text{-}CO)_3\{P(C_6H_{11})_3\}_4]$ [7] and in the phosphido- and sulphur dioxide-bridged bonds of $[Pt_3(\mu_2\text{-}Ph)(\mu_2\text{-}PPh_2)(\mu\text{-}SO_2)(PPh_3)_3]$ [9]. Unfortunately, no Pt–C distances are available for the orthorhombic modification of $[Pt_4(\mu_2\text{-}CO)_5(PMe_2Ph)_4]$.

The Pt–P distances determined herein are quite normal, and as expected are somewhat shorter for Pt(1) and Pt(4). Similarly there are no unusual parameters within the phosphine ligands.

In the present (monoclinic) modification of $[Pt_4(\mu_2\text{-}CO)_5(PMe_2Ph)_4]$, molecules occur pairwise, linked by a quasi-graphitic interaction between the phenyl ring C(33–38) and its (necessarily parallel) inverse at $-x, 1-y, -1-z$; the distance between ring centroids is 4.34 Å, well within the critical limit [10] of 4.7 Å. In the absence of any information about the packing of molecules in the orthorhombic modification, it is impossible to comment on the relative thermodynamic stabilities of the two arrangements.

NMR Spectroscopy

Although both modifications of $[Pt_4(\mu_2\text{-}CO)_5(PMe_2Ph)_4]$ show a 'butterfly'-type skeletal arrangement of platinum atoms and therefore should contain two types of phosphine ligands, solutions of the tetranuclear complexes of this type show only equivalent ^{31}P-resonances. For the complex with $L = PEt_3$ the ^{31}P spectrum is unchanged down to 183 K. Thus the assignment of the ^{31}P NMR spectra will be first attempted using a model based on a tetrahedral arrangement of Pt-atoms, each of which carries a phosphine ligand. Within this approximation we need only consider the isotopomers (I)–(V) shown below together with their relative abundances and NMR nomenclature (we will consider ^{31}P as A and M, and ^{195}Pt as X).

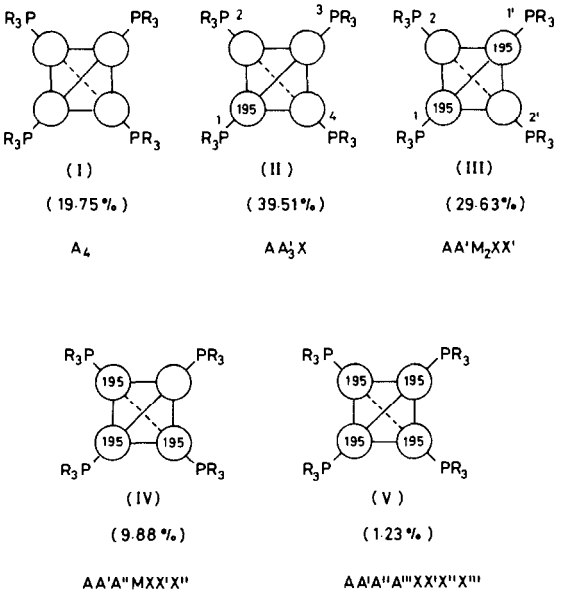

The ^{31}P *NMR spectrum* of $[Pt_4(\mu_2\text{-}CO)_5(PEt_3)_4]$ is shown in Fig. 2. Given the relative abundances of the isotopomers and our previous knowledge of the range of values for the coupling constants $^1J(^{195}Pt,^{31}P)$, $^1J(^{195}Pt,^{195}Pt)$, $^2J(^{195}Pt,^{31}P)$ and $^3J(^{31}P,^{31}P)$ in similar clusters [4, 5], we can seek those features of the observed spectrum which arise from the isotopomers (I)–(III). The signals from (IV) and (V) are too weak for a complete characterization; however, the data from (I)–(III) are sufficient to provide all of the relevant NMR parameters.

Isotopomer (I): The sub-spectrum due to this species is trivial and the expected singlet is observed at δ = 35.0 ppm.

Isotopomer (II): The resonances due to P^2–P^4 appear as a relatively intense doublet of doublets arising from $^2J(^{195}Pt,^{31}P)$ and $^3J(^{31}P,^{31}P)$ centred around the resonance of isotopomer (I) while those due to P^1 appear as a doublet of quartets, somewhat removed from the center bands because of the large value of $^1J(^{195}Pt,^{31}P)$.

Isotopomer (III): Here, P^2 will appear as a triplet of triplets, partially obscured by the resonance of (I), stemming from $^2J(^{195}Pt,^{31}P)$ and $^3J(^{31}P,^{31}P)$ (see Fig. 2a) whereas P^1 and $P^{1'}$ afford a complex second-order multiplet in the satellite region, from which we can calculate the platinum–platinum coupling constant (Fig. 2b).

With this somewhat simplified approach* one obtains reasonable estimates for all of the coupling

*The actual separations are the sum of several coupling constants.

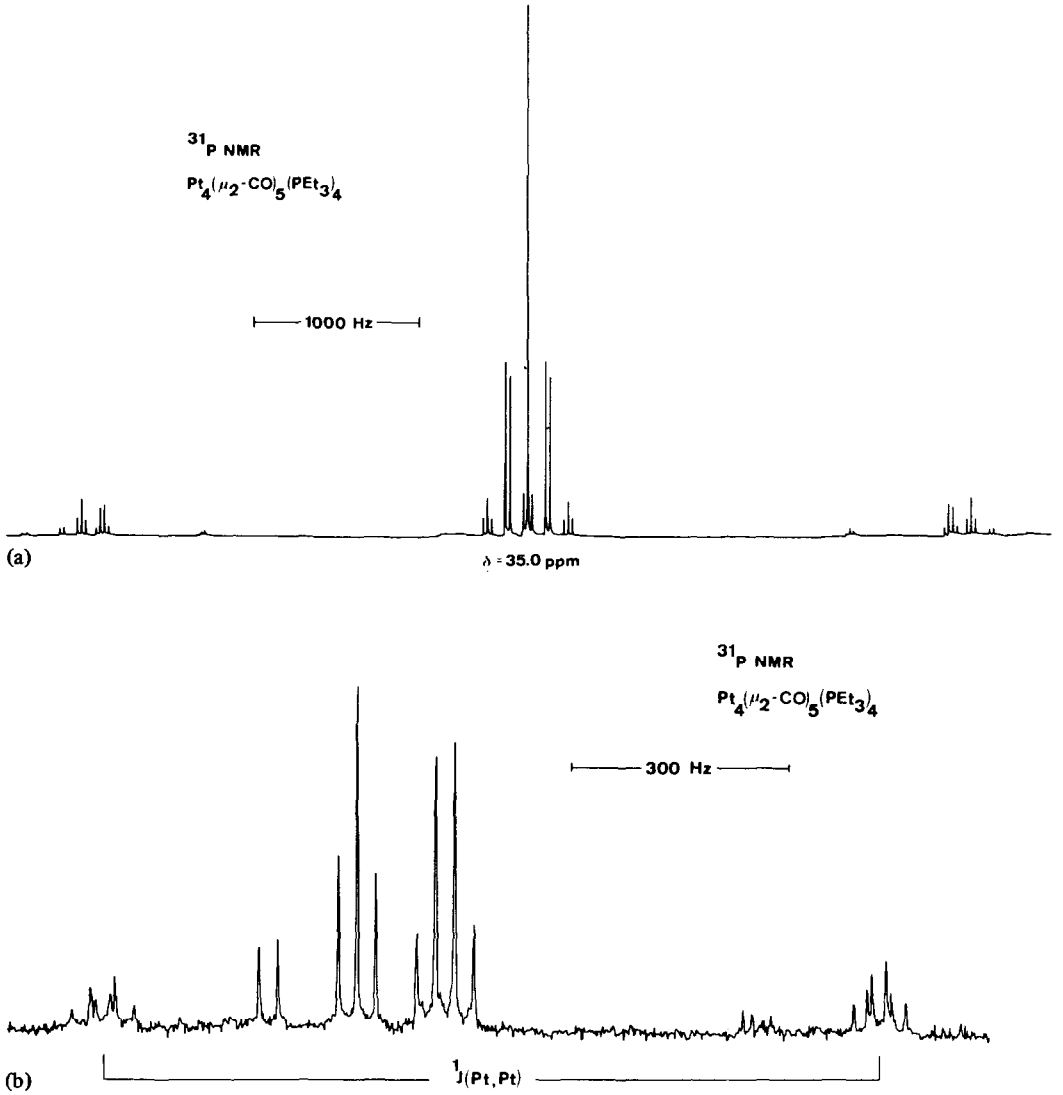

Fig. 2. (a) ^{31}P NMR spectrum of $[Pt_4(\mu_2\text{-}CO)_5(PEt_3)_4]$ in acetone-d_6 at room temperature. All four PEt_3 ligands are equivalent. (b) Expansion of the low field ^{195}Pt satellite region showing the signals arising from platinum-platinum coupling plus the various multiplicities due to the $^3J(^{31}P,^{31}P)$ coupling from (right to left) (II), (III) and (IV).

constants and computer simulation methods rapidly afford the necessary refinement. It is worth repeating [4, 5] that for *symmetrical* $\{Pt,P\}_n$ clusters, the ^{195}Pt satellites provide information about the nuclearity of the cluster since phosphorus bound to the ^{195}Pt couples with all remaining equivalent Pt-^{31}P fragments. Thus, for a Pt_4P_4 unit there will be (*1*) a *quartet* structure arising from the three P-atoms of isotopomer (II) which are *not* bound to ^{195}Pt, (*2*) a *triplet* structure in isotopomer (*III*) from the two phosphorus atoms not bound to ^{195}Pt, and (*3*) a *doublet* from the unique phosphorus atom of isotopomer (IV).

The ^{195}*Pt NMR spectrum* of $[Pt_4(\mu_2\text{-}CO)_5(PEt_3)_4]$ is shown in Fig. 3 and shows only one ^{195}Pt environment.

The metal chemical shift is in the expected region for such clusters [11], and does not depend significantly on the tertiary phosphine ligand. This spectrum seems somewhat more complicated than its ^{31}P analog due to the increased relative weights of (IV) and (V), but contains the same coupling constant information and has been satisfactorily reproduced *via* computer simulation.

The ^{13}*C spectrum* of $[Pt_4(\mu_2\text{-}CO)_5(PEt_3)_4]$ at room temperature shows a single CO environment with pentet multiplicity at $\delta = 222.1$ ppm resulting from rapid scrambling of the carbonyl ligands*.

A summary of the various NMR parameters for the *454* clusters is provided in Table IV, where:

*The spectral signal-to-noise is insufficient to permit a detailed analysis.

Fig. 3. ^{195}Pt NMR spectrum of $[Pt_4(\mu_2\text{-}CO)_5(PEt_3)_4]$ at room temperature in acetone-d_6.

TABLE IV. NMR Data for the Complexes $[Pt_4(\mu_2\text{-}CO)_5L_4]$.

L	$\delta^{31}P$	$\delta^{195}Pt$	$^1J(^{195}Pt,^{195}Pt)$	$^1J(^{195}Pt,^{31}P)$	$^2J(^{195}Pt,^{31}P)$	$^3J(^{31}P,^{31}P)$
PEt_3 [a]	35.0	−4180	1072	5118	244	26
PMe_2Ph [b]	10.3	−4162	1110	5260	260	27
$PMePh_2$ [c]	25.0	−4191	1124	5299	263	27
PEt_2Bu^t [d]	53.6			5074	240	27

[a]In acetone-d_6 at room temperature. [b]^{31}P in CH_2Cl_2/acetone-d_6 at 253 K, ^{195}Pt in CD_2Cl_2 at 218 K. [c]In CD_2Cl_2 at 253 K. [d]In CH_2Cl_2/C_6D_6 at 273 K.

a) $^1J(^{195}Pt,^{31}P)$ at 5074–5290 Hz is slightly larger than the 4412–4715 Hz range found for the *333* analogs (VI).

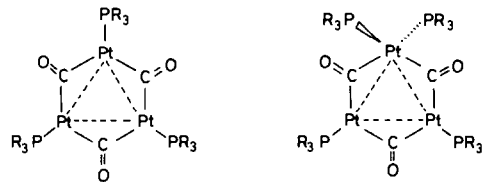

$[Pt_3(\mu_2\text{-}CO)_3(PR_3)_3]$ (VI) = 333

$[Pt_3(\mu_2\text{-}CO)_3(PR_3)_4]$ (VII) = 334

b) $^1J(^{195}Pt,^{195}Pt)$ (actually a sum of all Pt–Pt coupling pathways) at 1072–1124 Hz is considerably smaller than found for the complexes (VI) (1548–1790 Hz).

c) Both $^2J(^{195}Pt,^{31}P)$ and $^3J(^{31}P,^{31}P)$ are about half of that observed for the complexes (VI) but show a similarity to some values found in the compounds (VII).

d) The ^{31}P chemical shifts fall in the range δ = 10.3–53.6 ppm, generally at higher field than observed for the *333* derivatives, δ = 55.6–81.6 ppm.

In view of the complexity of our molecules, we decided to treat these NMR data empirically, beginning with the assumption that there is a low energy fluxional process occurring in solution. The sharp ^{31}P resonances and retention of $^{31}P,^{31}P$ multiplicity speak against phosphorus exchange processes. Although carbonyl exchanges must occur in solution, this process alone is insufficient to account for the observation of a single ^{195}Pt entity if the original butterfly structure is retained (note that in the solid state there are two chemically different Pt environments). Consequently, we favor a process involving Pt–Pt bond breaking and making and suggest that the 'butterfly' is 'flapping its wings' as shown below.

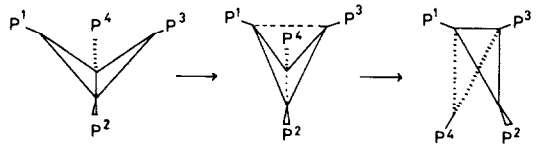

Thus the observed NMR data correspond to an average of these structures. Note that for isotopomer (II) if one assumed the planar symmetrical structure (VIII) one would *not* find quartet fine structure in the ^{195}Pt satellites unless the values $^4J(^{31}P,^{31}P)$ were accidentally equal to $^3J(^{31}P,^{31}P)$.

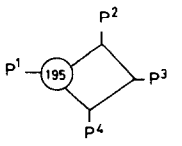

(VIII)

Additionally, in (VIII), the resonances for P^2 and P^3 should show two types of long-range $J(^{195}Pt,^{31}P)$ coupling constants, a ^2J to P^2 and a ^3J to P^3, and this is also not observed. Again it is conceivable that $^2J = {}^3J$; however, we feel that simultaneous coincidence of several very different types of coupling is unlikely. Moreover, these coincidences would have to be independent of phosphine, as we find the same NMR picture for all of our *454* complexes. If one assumes a tetrahedral model for the time-averaging one can also explain points b) and c) since during this process a small $J(P^1,P^4)$ and a larger $J(P^1,P^2)$ are being averaged. Similarly $J(Pt^1,Pt^4)$, if smaller than $J(Pt^1,Pt^2)$, will also contribute to a decrease in the overall J(Pt,Pt) values.

Although we are not certain what (if any) chemical significance should be attributed to the changes in ^1J and ^2J of platinum carbonyl phosphine clusters, it seems likely that we can continue to employ these data in an empirical way in the development of this cluster chemistry.

Experimental

Crystal Data

$C_{37}H_{44}O_5P_4Pt_4$, $M = 1473.01$, monoclinic, $a = 19.698(4)$, $b = 10.9440(20)$, $c = 21.360(6)$ Å, $\beta = 112.432(18)°$, $U = 4256(3)$ Å^3, $Z = 4$, $D_c = 2.299$ g cm^{-3}, $F(000) = 2712$, Mo-K_α X-radiation, $\lambda_{\alpha 1} = 0.70926$, $\lambda_{\alpha 2} = 0.71354$ Å, μ(Mo-$K_{\bar{\alpha}}$) = 127.8 cm^{-1}. Preliminary Weissenberg photographs showed systematic absences consistent with space group $P2_1/n$ (non-standard setting of $P2_1/c$, $C^5{}_{2h}$, No. 14).

Data Collection and Reduction

A single crystal, *ca.* 0.03 × 0.02 × 0.02 cm was mounted on a thin quartz fibre and set on an Enraf-Nonius CAD4 diffractometer. 25 reflections, $10 < \theta < 17°$, were accurately centred, and their setting angles used to determine, by least-squares, the accurate unit cell parameters and orientation matrix. Data collection employed $\theta - 2\theta$ scans in 96 steps, within the ranges $1.5 \leqslant \theta \leqslant 25.0°$ (graphite-monochromated Mo-K_α X-radiation), and $0 \leqslant h \leqslant 23$, $0 \leqslant k \leqslant 13$, $\bar{25} \leqslant l \leqslant 25$ (with equivalent 0kl and 0k$\bar{l}$ reflections afterwards merged). The θ scan rate was given by $0.8 + 0.35 \tan\theta$, and after rapid prescan only those reflections with $I \geqslant 2.0\ \sigma(I)$ were re-scanned at variable rate such that the final net intensity had $I \geqslant 33\ \sigma(I)$, subject to a 60 s maximum measuring time. Two intensity control and two orientation control reflections were re-measured every 3600 s and 100 reflections respectively, but subsequent analysis of their net intensities as individual functions of time revealed no crystal movement or decomposition, or machine variance, over the *ca.* 84 hr X-ray exposure.

Data were corrected for absorption (psi scans) and Lorentz and polarisation effects. Of 6253 symmetry-independent reflections measured (excluding those systematically absent) 4751 with $F_o \geqslant 2.0\ \sigma(F_o)$ were used to solve and refine the structure.

Solution and Refinement

The positions of the platinum atoms were determined by automatic centrosymmetric direct methods, whilst an interactive combination of full-matrix least-squares refinement and difference Fourier syntheses were used to locate all others. The carbon atoms of phenyl groups were refined as regular, planar hexagons, C–C = 1.395 Å, but with independent thermal parameters. Phenyl hydrogen atoms were set in idealized positions and allowed to ride on their respective carbons, with C–H = 1.08 Å and $U_H = 0.1$ Å^2. No contribution to F_c from methyl hydrogen atoms was included.

Structure factors were weighted according to $w^{-1} = [\sigma^2(F_o) + 0.0031\ (F_o)^2]$, a scheme that afforded no unusual or systematic variation of the root mean square deviation of a reflection of unit weight *versus* parity group, $(\sin\theta)/\lambda$, F_o, h, k, or l. In the final stages of refinement Pt and P atoms were allowed anisotropic thermal motion. At convergence, $R = 0.0846$, $R_w = 0.0908$ for 193 variables. The maximum residue revealed by an ultimate difference Fourier was *ca.* 2.1 e Å^{-3}, 1 Å from Pt(I), and is presumably a consequence of the inadequacy of the absorption correction. In view of this, parallel refinement using uncorrected data was performed, but yielded significantly poorer results. We are therefore confident that, whilst clearly not perfect, the applied correction has at least some merit.

All crystallographic calculations were performed with the SHELX76 [12] and XANADU [13] programs on the University of London Computer CDC 7600 computer, using inlaid neutral atom scattering factors for P, O, C and H, and, for Pt, coefficients for an analytical approximation taken from 'International Tables' [14]. The final positional and thermal parameters obtained are listed in Table I. A comparison of $10|F_o|$ *vs* $10\ F_c$ at the termination of refinement has been deposited with the Editor, together with H-atom positional parameters. Figure 1 was constructed using ORTEP-II [15].

NMR Spectra

^{31}P, ^{195}Pt and ^{13}C NMR spectra were measured using Bruker HX-90 and WM-250 NMR spectrometers as described previously [4, 5] using external H_3PO_4, external Na_2PtCl_6 and internal TMS as reference materials. Coupling constants are estimated to be ±3 Hz, chemical shifts ±0.1 ppm. The ^{31}P NMR spectra revealed broad unresolved signals due to the presence of small quantities of the compounds

TABLE V. IR and Microanalytical Data for the Complexes $[Pt_4(\mu_2\text{-}CO)_5L_4]$.

L	Carbonyl stretching vibrations (nujol) cm^{-1}.	Microanalytical data: calc. (found) C	H	P
PMe_2Ph	1800s, 1784vs, 1768s	30.17 (29.92)	3.01 (2.92)	8.41 (8.74)
PEt_3	1840shw, 1788vs	25.00 (25.11)	4.34 (4.19)	8.99 (8.70)
PEt_2Bu^t	1837vw, 1805s, 1788vs, 1776vs	29.52 (30.58)	5.09 (5.17)	8.23 (8.55)

$[Pt_3(\mu_2\text{-}CO)_3(\text{tertiary phosphine})_4]$. Spectral simulations were performed using the program PANIC.

The ligands and starting complexes were obtained as in refs. 4 and 5. $[Pt(1,5\text{-}COD)_2]$ was obtained from Emser Werke, Zürich. Microanalytical and IR data for the complexes are shown in Table V.

$[Pt_4(\mu_2\text{-}CO)_5(PMe_2Ph)_4]$

$[Pt_3(\mu_2\text{-}CO)_3(PMe_2Ph)_4]$ (1 g, $8.2\cdot10^{-4}$ mol) was dissolved in 70 ml of boiling methanol under a carbon monoxide atmosphere. The solution was then filtered hot and cooled after which $[Pt_4(\mu_2\text{-}CO)_5(PMe_2Ph)_4]$ crystallized as purple plates (0.59 g, 65%).

$[Pt_4(\mu_2\text{-}CO)_5(PEt_3)_4]$

$[Pt(1,5\text{-}COD)_2]$ (0.21 g, $5\cdot10^{-4}$ mol) was dissolved in 15 ml petroleum ether under ethylene at 0 °C. Addition of PEt_3 (0.1 ml, $6.8\cdot10^{-4}$ mol) followed by saturation with carbon monoxide and standing for 30 min. resulted in a dark red solution. Removal of the solvent in vacuum, extraction of the residue with boiling methanol followed by cooling gave $[Pt_4(\mu_2\text{-}CO)_5(PEt_3)_4]$ as dark violet needles (0.10 g, 57%).

$[Pt_4(\mu_2\text{-}CO)_5(PEt_2Bu^t)_4]$

The procedure described for $[Pt_4(\mu_2\text{-}CO)_5(PEt_3)_4]$ was followed except that the extraction was performed with 3 ml of hot toluene in a carbon monoxide atmosphere. Addition of methanol afforded $[Pt_4(\mu_2\text{-}CO)_5(PEt_2Bu^t)_4]$ as dark violet crystals. From $[Pt(COD)_2]$ (0.42 g, 10^{-3} mol) and PEt_2Bu^t (0.18 ml, 10^{-3} mol) 0.23 g (61%) of product was obtained.

Acknowledgement

We thank the ETH Zürich and the Swiss National Science Foundation for support.

References

1 J. C. Calabrese, L. F. Dahl, A. Cavalieri, P. Chini, G. Longoni and S. Martinengo, *J. Am. Chem. Soc., 96*, 2614 (1974); N. J. Taylor, P. C. Chieh and A. J. Carty, *J.C.S. Chem. Comm.*, 448 (1975); A. Albinati, A. Moor, P. S. Pregosin and L. M. Venanzi, *J. Am. Chem. Soc., 104*, 7672 (1982).
2 F. G. Stone, *Acc. Chem. Res., 14*, 318 (1981); F. G. Stone, *Inorg. Chim. Acta, 50*, 33 (1981); M. Green, K. A. Mead, R. M. Mills, I. D. Salter, F. G. A. Stone and P. Woodward, *J.C.S. Chem. Comm.*, 51 (1982); P. W. Frost, J. K. Howard, J. L. Spencer, D. G. Turner and D. Gregson, *J.C.S. Chem. Comm.*, 1104 (1981).
3 P. Braunstein, J. Jud, Y. Dusausoy and J. Fischer, *Organomet., 2*, 180 (1983); P. Bender and P. Braunstein, *J.C.S. Chem. Comm.*, 334 (1983); J. P. Barbier, R. Bender, P. Braunstein, J. Fischer and L. Ricard, *J. Chem. Res. (S)*, 230 (1978); R. Bender, P. Braunstein, Y. Dusausoy and J. Protas, *J. Organometal. Chem., 172*, C51 (1979).
4 A. Moor, P. S. Pregosin and L. M. Venanzi, *Inorg. Chim. Acta, 48*, 153 (1981).
5 A. Moor, P. S. Pregosin and L. M. Venanzi, *Inorg. Chim. Acta, 61*, 135 (1982).
6 R. G. Vranka, L. F. Dahl, P. Chini and J. Chatt, *J. Am. Chem. Soc., 91*, 1574 (1969).
7 A. Albinati, G. Carturan and A. Musco, *Inorg. Chim. Acta, 16*, L3 (1976).
8 A. Albinati, *Inorg. Chim. Acta, 22*, L31 (1977).
9 D. G. Evans, G. R. Hughes, D. M. P. Mingos, J.-M. Bassett and A. J. Welch, *J. C. S. Chem. Comm.*, 1255 (1980).
10 A. J. Welch, *Ph.D. Thesis, University of London*, England (1974).
11 P. S. Pregosin, *Coord. Chem. Rev., 44*, 247 (1982).
12 G. M. Sheldrick, *'SHELX76', University Chemical Laboratory, Cambridge*, England (1976).
13 P. Roberts and G. M. Sheldrick, *'XANADU', University Chemical Laboratory, Cambridge*, England (1976).
14 *International Tables for X-Ray Christallography*, Vol. 4, Kynoch Press, Birmingham, England (1974).
15 C. K. Johnson, *'ORTEP-II', Report ORNL-5138, Oak Ridge National Laboratory, Tennessee*, U.S.A. (1976).